

# The Simplest Oscillon and its Sphaleron

N. S. Manton<sup>1,\*</sup> and T. Romańczukiewicz<sup>2,†</sup>

<sup>1</sup>*Department of Applied Mathematics and Theoretical Physics,  
University of Cambridge, Wilberforce Road, Cambridge CB3 0WA, U.K.*

<sup>2</sup>*Institute of Theoretical Physics, Jagiellonian University, Łojasiewicza 11, Kraków, Poland*

Oscillons in a simple, 1-dimensional scalar field theory with a cubic potential are discussed. The theory has a classical sphaleron, whose decay generates a version of the oscillon. A good approximation to the small-amplitude oscillon is constructed explicitly using the asymptotic expansion of Fodor et al., but for larger amplitudes a better approximation uses the discrete, unstable and stable deformation modes of the sphaleron.

## I. INTRODUCTION

Oscillons are spatially-localised, long-lived, oscillatory solutions of the field equation(s) of classical field theories [1]. The nonlinearity of the field equation is essential. Oscillons, unlike kinks and other types of classical soliton, have no topological charge ensuring their stability, and it is surprising that oscillons do not couple more strongly to radiation modes of the field, leading to rapid decay towards the classical vacuum.

Despite oscillons being known in a variety of field theories in various spatial dimensions, the fundamental reason for their existence remains somewhat mysterious. We will show that, at least for the special, simple oscillon that we consider here in detail, the oscillon can be thought of as a decaying sphaleron of the field theory. By a sphaleron, we mean a localised, static but unstable solution of the field equation [2].

For an oscillon to exist, the continuum of radiation modes of the linearised field needs to have a frequency gap, starting at some positive threshold frequency  $m$ . A basic oscillon is periodic, with a fundamental frequency  $\omega < m$ , so it couples to radiation only through

\* [N.S.Manton@damtp.cam.ac.uk](mailto:N.S.Manton@damtp.cam.ac.uk)

† [tomasz.romanczukiewicz@uj.edu.pl](mailto:tomasz.romanczukiewicz@uj.edu.pl)

nonlinear terms, at frequencies that are multiples of  $\omega$ . The oscillon has an arbitrary amplitude lying in some finite range upwards from zero, and as the amplitude increases, the frequency  $\omega$  decreases away from the threshold  $m$ . Generally,  $2\omega$  and higher integer multiples of  $\omega$  are in the continuum (although some exceptions are known [3]), which underlines the surprise that the oscillon is so long-lived. Nevertheless, an oscillon does slowly radiate energy away, and as it does so its amplitude decreases and its frequency increases.

Much of the understanding of oscillons comes from numerical investigation. One prototype is the oscillon in  $\phi^4$  scalar field theory, where the field potential is of the familiar double-well form. This oscillon exists in the theory in 1-, 2- or 3-dimensions, with the field profile depending just on radius and time (up to a spatial translation). In the 1-dimensional theory, the oscillon is reflection-symmetric about the origin. An oscillon of this type is produced by starting from generic initial conditions of the form of a symmetric hump, for example a Gaussian shape, superimposed on one of the vacua. Oscillon formation is rather robust, and the initial shape is not very important. There is usually a transient in which the field shape changes over one or two oscillations, with pulses of energy being radiated to the left and right, and then the field settles into the oscillon.

A substantial theoretical analysis of oscillon structure was given by Fodor et al. [4], for oscillons of small and modest amplitude<sup>1</sup>. These authors considered a rather general scalar field theory in spatial dimension  $D \leq 3$ , whose potential  $V(\phi)$  has a Taylor expansion in  $\phi$  about a quadratic minimum at  $\phi = 0$ . By an iterative method, using the field equation, they systematically constructed an oscillon as a series in an expansion parameter  $\epsilon$ , related to the amplitude. The oscillon's existence depends on the strength of the cubic and higher-power terms in  $V$ , but the conditions that arise are inequalities, so oscillons are generic for small  $\epsilon$ . By construction, the oscillon depends just on radius and on time, and it is periodic (i.e. the Fourier series w.r.t. time has terms that are multiples of a unique, fundamental frequency  $\omega$ ).

We shall use the method of Fodor et al. to explicitly construct a particularly simple oscillon in 1-dimension. In practice, the algebra is still quite tricky, and we have only found the first four terms of the series in  $\epsilon$ . As is hardly surprising, this series is asymptotic rather than convergent, because if the series were convergent then there would be a strictly-periodic, exact oscillon solution, having infinite lifetime. In practice, for small  $\epsilon$  it is useful to sum

---

<sup>1</sup> Refs. [1] and [4] comprehensively review the oscillon literature up to 2009.

all four terms to obtain a good approximation to the oscillon, but as  $\epsilon$  and the amplitude increase, one needs to truncate the series after fewer terms, as is typical for asymptotic series; the discarded terms are larger than the last retained term.

For oscillons of even larger amplitude, the method of Fodor et al. tends to break down, but instead, the oscillon can now be interpreted as arising from the decay of a static sphaleron solution. The decaying sphaleron can be well approximated using an ansatz constructed from two discrete modes of the linearised deformations of the sphaleron, one unstable and the other stable. This analysis shows that the sphaleron can be regarded as the precursor of the oscillon.

The study of oscillons in field theories with double-well minima has tended to hide this proposed connection between sphalerons and oscillons. For example, the  $\phi^4$  theory in 1-dimension with double-well potential has no true sphaleron, but it has the configuration of a kink and antikink at infinite separation as a ‘sphaleron’. If a kink and antikink are released from a large separation at zero velocity, and evolved numerically, then they turn into an oscillon (often called a bion in this context). The sine-Gordon breather [5] provides another example. This is an oscillon that lasts indefinitely because of exact integrability. A large-amplitude breather instantaneously comes to rest resembling a kink and antikink at large separation. Again, the kink-antikink configuration at infinite separation can be thought of as a sphaleron. The sine-Gordon breather exhibits a key property of an oscillon, namely, that its fundamental frequency is less than the continuum threshold for linearised waves, and as its amplitude increases, the frequency decreases away from this threshold.

The connection between oscillons and sphalerons is clearer if there is a genuine sphaleron of finite size in the field theory. Here, we focus on a scalar field theory in 1-dimension which has such a sphaleron. We assume that  $V(\phi)$  has a quadratic minimum at  $\phi = 0$ , with  $V(0) = 0$ . Then, a sphaleron exists if  $V$  becomes negative for some  $\phi > 0$ . (It is convenient to choose this sign for the inequality, but  $\phi < 0$  is equivalent.) More simply, we assume that  $V(\phi)$  increases to a local maximum at  $\phi = \phi_1 > 0$ , then decreases and passes linearly through  $V = 0$  at some  $\phi_2 > \phi_1$ .  $V$  could have further local or global minima as  $\phi$  increases further. Note that  $\phi = 0$ , which is the asymptotic value of the sphaleron tail field, is a *false* vacuum, because it is not the global minimum of  $V$ , but this doesn’t cause difficulties.

The existence of a time-independent sphaleron solution in 1-dimension can be easily understood using the standard trick of identifying the static field equation as the equation

for a particle rolling in the inverted potential  $-V$ . In the inverted potential, the particle starts at rest from  $\phi = 0$ , rolls through the potential minimum at  $\phi = \phi_1$  and ascends the potential to  $\phi_2$ . As the potential is linear here, the particle stops instantaneously, then rolls back to the starting point at  $\phi = 0$ . Because  $V$  is quadratic around  $\phi = 0$ , the whole process takes infinite time. Spatially, one obtains a hump-shaped sphaleron profile which has field values lying in the range  $0 < \phi \leq \phi_2$ , with tails approaching  $\phi = 0$  exponentially fast.

The connection between oscillons and sphalerons in a potential of this type seems first to have been noted in ref.[6], but here we will explore the connection more systematically. We will work with the simplest potential of the required form, the purely cubic potential  $V(\phi) = \frac{1}{2}\phi^2 - \frac{1}{3}\phi^3$ .  $V$  has a quadratic local minimum at  $\phi = 0$ , with value zero, a local maximum at  $\phi_1 = 1$ , and passes through zero linearly at  $\phi_2 = \frac{3}{2}$ . The sphaleron has a simple analytical form, and we can calculate its unstable mode, its translation zero mode, and its single discrete vibrational mode – its shape mode. At the same time, this potential allows for explicit calculation of a small-amplitude oscillon as a series, using the method of Fodor et al., and we have analytically calculated the terms up to fourth order in the expansion parameter  $\epsilon$ . Importantly, we will show numerically that if the sphaleron is perturbed by its unstable mode, in the direction of decreasing  $\phi$ , then it evolves into the oscillon. (If it is perturbed in the opposite direction, then the field values quickly become very large, and the field becomes singular.)

This sphaleron in 1-dimension, arising from a cubic potential, is not new. It occurs as a “bounce” in work of Callan and Coleman [7] and was discussed in detail by Avelar et al. [8]. These authors noted that because its translation zero mode has a node, there must be a mode with negative squared frequency, i.e. an instability. Avelar et al. also found the positive-frequency shape mode. However, the connection to oscillons appears not to have been investigated before.

Clearly, at the linearised level, the instability and shape oscillation of the sphaleron can be modelled by combining the sphaleron with the two relevant discrete modes. As we shall only consider the sphaleron and oscillon with their centres of mass at rest, we can ignore the translation zero mode. The perturbed sphaleron, like the oscillon, is then reflection-symmetric. We shall now make a bold leap, and consider the sphaleron deformed by these two modes with arbitrarily large, time-dependent amplitudes. This is a collective coordinate ansatz for the evolution of the sphaleron. The reduced, collective coordinate Lagrangian,

obtained by substituting this ansatz into the field-theoretic Lagrangian, is nonlinear but rather simple. We will show that its resulting dynamics gives another good approximation to the oscillon, which is particularly useful when the oscillon has quite large amplitude and the series of Fodor et al. breaks down.

We should clarify here that the oscillon constructed by the method of Fodor et al. has just one degree of freedom, its amplitude, and its shape and frequency depend on this. Numerically however, one typically finds that an oscillon appears to be quasi-periodic, although by careful adjustment of initial conditions, the periodic version can be found too. To model quasi-periodic behaviour one needs to have a system with two degrees of freedom at least, and the two mode amplitudes of the deformed sphaleron provide these. This issue was also recently raised by Blaschke and Karpíšek [9], who studied a mechanised model of an oscillon with two internal degrees of freedom (in addition to the centre of mass position). In fact, a non-integrable Lagrangian system with two degrees of freedom (and 4-dimensional phase space) has more complicated dynamics than quasi-periodic motion, but we have not been able to observe this in the oscillon. The issue of quasi-periodic or chaotic behaviour of the oscillon is complicated, because the reduced system is only an approximation to the field theory with its infinitely many degrees of freedom, and does not couple to radiation.

It is surprising that a model using the sphaleron's two linearised modes is quantitatively useful, because there are no values of the two mode amplitudes giving the vacuum field configuration  $\phi \equiv 0$  exactly (although, for optimal values, it gets quite close). Consequently, this rather crude model cannot accurately describe oscillons of small amplitude.

In the following, we introduce the scalar field theory with cubic potential, then construct the first four terms in the series for the small-amplitude oscillon solution, following Fodor et al. Next, we recall the sphaleron solution and its discrete modes, and use these to construct and test our collective coordinate dynamics modelling an oscillon of larger amplitude. Finally, we describe in further detail some features of the oscillon that we have uncovered numerically, and present our conclusions.

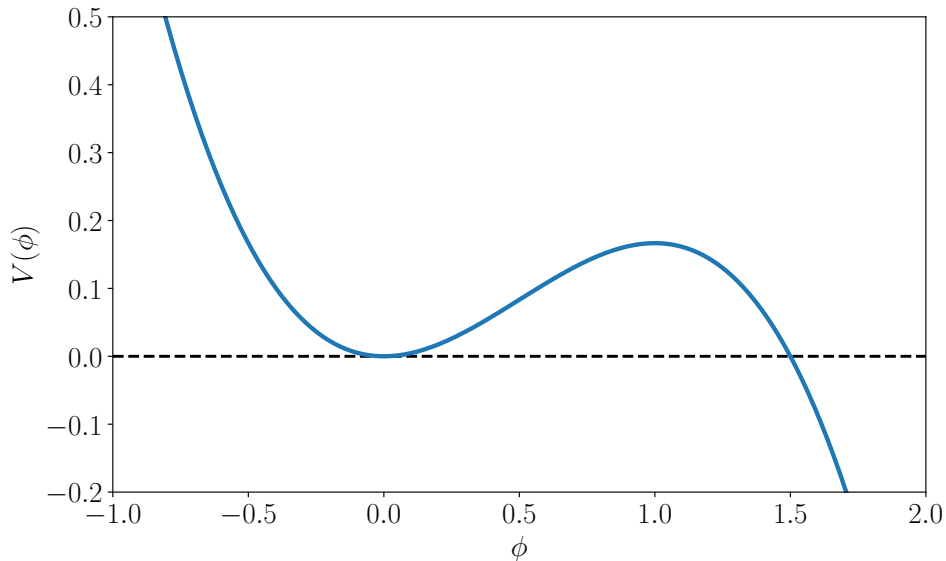


FIG. 1: Potential  $V(\phi) = \frac{1}{2}\phi^2 - \frac{1}{3}\phi^3$ .

## II. A SIMPLE SCALAR FIELD THEORY

Consider the theory for a real scalar field  $\phi(t, x)$  in 1-dimension, with Lagrangian

$$L[\phi] = \int_{-\infty}^{\infty} \left( \frac{1}{2}\phi_t^2 - \frac{1}{2}\phi_x^2 - \frac{1}{2}\phi^2 + \frac{1}{3}\phi^3 \right) dx. \quad (1)$$

This has the simple nonlinear field equation

$$\phi_{tt} - \phi_{xx} + \phi - \phi^2 = 0. \quad (2)$$

FIG. 1 shows the potential

$$V(\phi) = \frac{1}{2}\phi^2 - \frac{1}{3}\phi^3, \quad (3)$$

which is unbounded below but has a local quadratic minimum at  $\phi = 0$  with  $V(0)$  zero, and a local maximum at  $\phi = 1$  with  $V(1) = \frac{1}{6}$ . Additionally,  $V$  passes linearly through zero at  $\phi = \frac{3}{2}$ .

## III. THE SMALL-AMPLITUDE OSCILLON

Following the method of Fodor et al. [4] to construct an oscillon solution of eq.(2), we expand the field in powers of a small parameter  $\epsilon$ ,

$$\phi = \sum_{k=1}^{\infty} \epsilon^k \phi_k(t, x). \quad (4)$$

We denote the truncated series as  $\Phi_N = \sum_{k=1}^N \epsilon^k \phi_k(t, x)$ . We also introduce rescaled space and time variables

$$\zeta = \epsilon x, \quad \tau = \omega t \quad (5)$$

and assume that

$$\omega = \sqrt{1 - \epsilon^2}, \quad (6)$$

which locks the expansion parameter  $\epsilon$  to the oscillon frequency. We assume the oscillon is instantaneously at rest at  $\tau = 0$ , so it is symmetric in  $\tau$ . The oscillon will also be symmetric in  $\zeta$ , and we can identify its amplitude as  $\sum_{k=1}^{\infty} \epsilon^k \phi_k(0, 0)$ , or the truncated version of this. In terms of these new variables the field equation (2) takes the form

$$(1 - \epsilon^2)\ddot{\phi} - \epsilon^2\phi'' + \phi - \phi^2 = 0, \quad (7)$$

where overdots and primes denote derivatives w.r.t.  $\tau$  and  $\zeta$  respectively. Expanding in powers of  $\epsilon$ , we obtain an infinite set of coupled equations, of which the first five are

$$\ddot{\phi}_1 + \phi_1 = 0, \quad (8)$$

$$\ddot{\phi}_2 + \phi_2 = \phi_1^2, \quad (9)$$

$$\ddot{\phi}_3 + \phi_3 = \ddot{\phi}_1 + \phi_1'' + 2\phi_1\phi_2, \quad (10)$$

$$\ddot{\phi}_4 + \phi_4 = \ddot{\phi}_2 + \phi_2'' + 2\phi_1\phi_3 + \phi_2^2, \quad (11)$$

$$\ddot{\phi}_5 + \phi_5 = \ddot{\phi}_3 + \phi_3'' + 2\phi_1\phi_4 + 2\phi_2\phi_3. \quad (12)$$

These can be regarded as an iterative sequence of ordinary, linear differential equations for  $\phi_1, \phi_2, \phi_3, \dots$ , whose sources on the right-hand side depend on the previously determined functions. [Note that in ref.[4], eqs.(11) and (12) are not given explicitly, and their version of eq.(10) has a typo; their explicit  $-\ddot{\phi}_1$  should be left out, as it is present in the term  $\omega_2\ddot{\phi}_1$ .]

The solution of eq.(8), symmetric in  $\tau$ , is

$$\phi_1 = p_1(\zeta) \cos \tau \quad (13)$$

where  $p_1$  is yet to be determined. Equation (9) now becomes  $\ddot{\phi}_2 + \phi_2 = \frac{1}{2}p_1^2(\zeta)(1 + \cos 2\tau)$ , whose solution, combining the particular integral with a homogeneous function symmetric in  $\tau$ , is

$$\phi_2 = p_2(\zeta) \cos \tau + \frac{1}{6}p_1^2(\zeta)(3 - \cos 2\tau). \quad (14)$$

The two unknown functions,  $p_1$  and  $p_2$ , are determined by considering eqs.(10) and (11) for  $\phi_3$  and  $\phi_4$ . First, for the oscillon to be periodic, there is a condition of *no resonance*, i.e. the right-hand side of eq.(10) should have no  $\cos \tau$  term. This condition reduces to

$$p_1'' - p_1 + \frac{5}{6}p_1^3 = 0, \quad (15)$$

whose solution symmetric in  $\zeta$ , and decaying for large  $|\zeta|$ , is

$$p_1(\zeta) = \sqrt{\frac{12}{5}} \frac{1}{\cosh \zeta}. \quad (16)$$

Second, one finds that it is consistent to set  $p_2 \equiv 0$ . This can be argued in more than one way. After solving for  $\phi_3$ , it is found that the no resonance condition for  $\phi_4$  implies that  $p_2$  obeys a linear differential equation whose solution is an antisymmetric function of  $\zeta$ , whereas we require the oscillon to be symmetric in  $\zeta$ . Setting  $p_2 \equiv 0$  also means that the oscillon can be symmetric under the combined transformations  $\epsilon \rightarrow -\epsilon$ ,  $\tau \rightarrow \tau + \pi$ . More generally, the latter symmetry requires that  $\phi_k$  only has terms  $\cos n\tau$  with  $n$  even/odd when  $k$  is even/odd. In summary, we have established that the leading terms in the series for the oscillon are

$$\phi_1 = \sqrt{\frac{12}{5}} \frac{\cos \tau}{\cosh \zeta}, \quad \phi_2 = \frac{2}{5} \frac{3 - \cos 2\tau}{\cosh^2 \zeta}. \quad (17)$$

Equation (10) now simplifies, and its solution is

$$\phi_3 = p_3(\zeta) \cos \tau + \sqrt{\frac{12}{5}} \frac{1}{20} \frac{\cos 3\tau}{\cosh^3 \zeta}, \quad (18)$$

where  $p_3$ , the homogeneous contribution, is as yet arbitrary and will not be zero. It is then straightforward to substitute for  $\phi_1, \phi_2$  and  $\phi_3$  in eq.(11), and integrate to find that

$$\phi_4 = \sqrt{\frac{12}{5}} \frac{1}{3} \frac{p_3(\zeta)}{\cosh \zeta} (3 - \cos 2\tau) + \frac{24}{5} \frac{1}{\cosh^2 \zeta} - \frac{1}{75} \frac{426 + 39 \cos 2\tau + \cos 4\tau}{\cosh^4 \zeta}. \quad (19)$$

There could be an additional homogeneous term  $p_4(\zeta) \cos \tau$ , but the symmetry mentioned above requires  $\phi_4$  only to have terms proportional to  $\cos n\tau$  with  $n$  even, so we can set  $p_4 \equiv 0$ .

Finally, we impose the no resonance condition for  $\phi_5$ , i.e. that there is no  $\cos \tau$  term on the right-hand side of eq.(12). This gives an ordinary differential equation for  $p_3$ , of the Pöschl–Teller form with a source, whose acceptable solution is

$$p_3(\zeta) = \sqrt{\frac{12}{5}} \frac{1}{60} \left( \frac{94}{\cosh \zeta} - \frac{119}{\cosh^3 \zeta} \right). \quad (20)$$



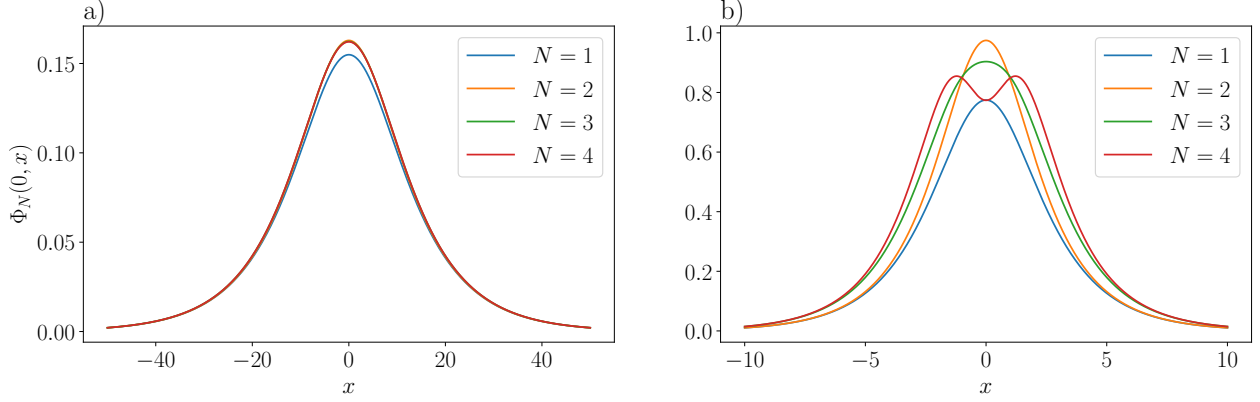


FIG. 2: Profiles of the oscillons at  $\tau = 0$  for truncation orders  $N = 1, \dots, 4$  of the Fodor et al. series – a)  $\epsilon = 0.1$  and b)  $\epsilon = 0.5$ .  $x$  is the unscaled spatial variable.

Combined with the earlier results (18) and (19), this gives the final form for  $\phi_3$  and  $\phi_4$ ,

$$\begin{aligned} \phi_3 &= \sqrt{\frac{12}{5}} \frac{1}{60} \left( \frac{94 \cos \tau}{\cosh \zeta} - \frac{119 \cos \tau - 3 \cos 3\tau}{\cosh^3 \zeta} \right), \\ \phi_4 &= \frac{1}{75} \left( \frac{642 - 94 \cos 2\tau}{\cosh^2 \zeta} - \frac{783 - 80 \cos 2\tau + \cos 4\tau}{\cosh^4 \zeta} \right). \end{aligned} \quad (21)$$

We do not calculate  $\phi_5$  as this will involve yet another non-zero arbitrary function  $p_5$  that can only be determined by a no resonance condition in the equation for  $\phi_7$ .

The truncated approximate oscillon,  $\Phi_N$ , is the sum of the first  $N$  terms of the expansion (4), where  $\phi_1, \dots, \phi_4$  are as in eqs.(17) and (21). FIGS. 2 show this truncated oscillon at  $\tau = 0$  for  $N = 1, \dots, 4$ , and for amplitude parameters  $\epsilon = 0.1$  and  $\epsilon = 0.5$ . FIG. 3 a) shows the combined strength of the contributing terms, evaluated at  $\zeta = \tau = 0$ . It is clear that for  $\epsilon \gtrsim 0.6$ , the higher-order terms are no longer small compared to the lower-order terms, as is typical for an asymptotic series, so it is better to truncate the series after two or three terms, obtaining  $\Phi_2$  or  $\Phi_3$ . The pronounced double-hump of the oscillon profile for large  $\epsilon$  in FIG. 3 b) appears therefore to be exaggerated, and not a reliable feature.

The truncated oscillon has just one degree of freedom,  $\epsilon$ , and it is periodic with  $t$ -period  $2\pi/\sqrt{1-\epsilon^2}$ . This is because of the symmetry assumptions that have been imposed. There were opportunities to include less symmetric terms in the construction, so a larger family of oscillons could probably be found, although more algebraic work would be required. There is therefore no inconsistency with the approach discussed below, where the oscillon is generally quasi-periodic.

To show the quality of the truncated oscillon, we have numerically solved the field

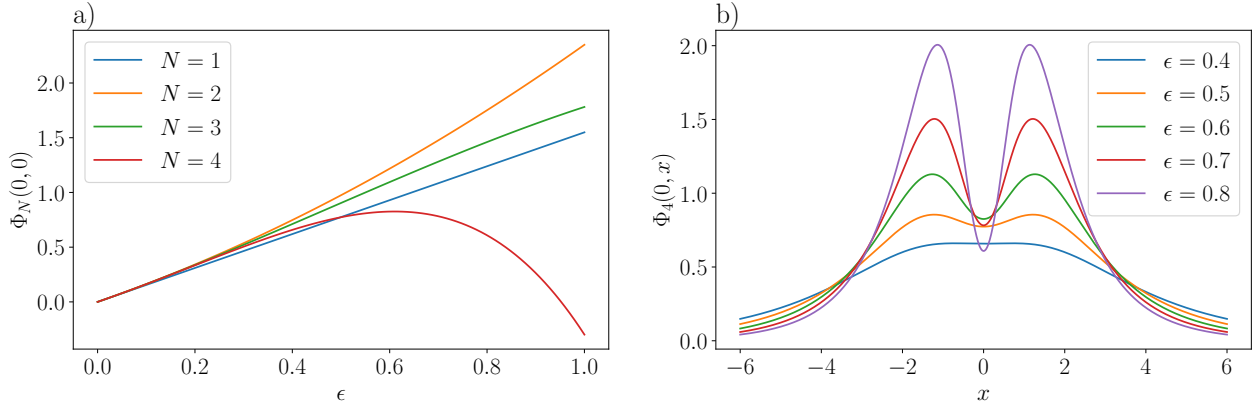


FIG. 3: a) Value of the field profile  $\Phi_N$  at the center  $\zeta = 0, \tau = 0$  for varying  $\epsilon$ . b) Profile of the truncated oscillon  $\Phi_4$  for larger values of  $\epsilon$ .

equation (using variables  $t, x$ ) with initial condition  $\Phi_N(0, x)$  for  $N = 1, \dots, 4$  and a wide range of  $\epsilon \in [0.1, 0.8]$ . We have measured the loss of energy from the spatial interval  $-100 < x < 100$  during the time interval  $0 < t < T = 300$ . The energy loss  $\Delta E$  is the time-integrated energy flux through the ends, which is equal on the left and right, so

$$\Delta E = 2 \int_0^T \phi_t(t, 100) \phi_x(t, 100) dt, \quad (22)$$

and is shown in FIG. 4. In the range  $\epsilon \in [0.1, 0.5]$ ,  $\Phi_3$  is the best initial condition. For larger  $\epsilon$ , the initial configuration  $\Phi_4$  loses energy faster, and the approximate oscillon  $\Phi_4(t, x)$  breaks down.  $\Phi_4$  is probably a better approximation to the numerical solution than  $\Phi_3$  for small values of  $\epsilon$ , but this is not clear from the figure because of possible numerical errors.

#### IV. THE SPHALERON

There exists a nontrivial, lump-like static solution of the field equation (2),

$$\phi_S(x) = \frac{3}{2} \frac{1}{\cosh^2 \frac{1}{2}x}. \quad (23)$$

This is expressed in terms of the unscaled spatial variable  $x$  and satisfies the boundary conditions  $\phi_S \rightarrow 0$  as  $x \rightarrow \pm\infty$ , like the oscillon. The solution can be translated, but as given, it is reflection-symmetric in  $x$ . Its energy is  $E = \frac{6}{5}$ .

A small perturbation  $\delta\phi = e^{i\omega t}\eta(x)$  of  $\phi_S$ , with frequency  $\omega$ , obeys the linearised equation

$$-\eta''(x) + U(x)\eta(x) = \omega^2\eta(x), \quad (24)$$

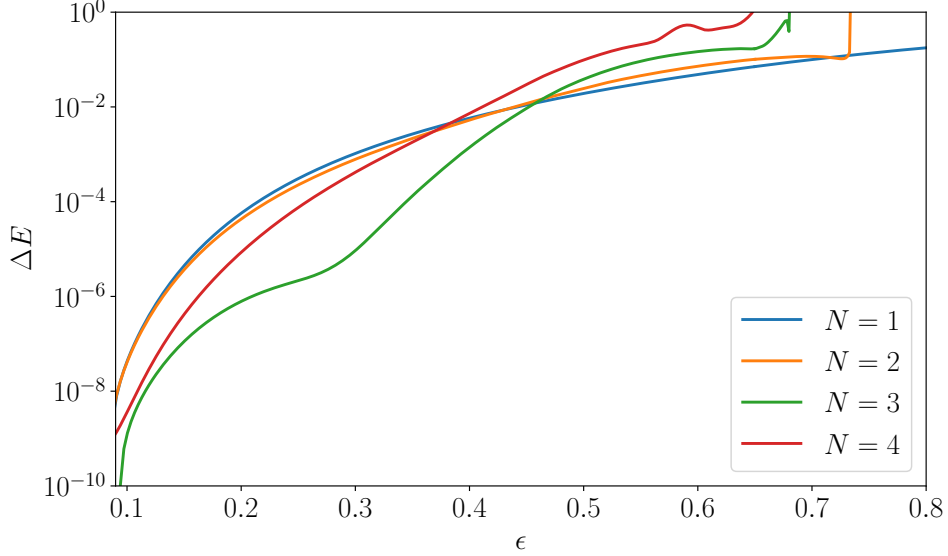


FIG. 4: Oscillon energy loss from the spatial interval  $[-100, 100]$  during time  $0 < t < 300$ , starting from the truncated series  $\Phi_N(0, x)$  as initial configuration.

where

$$U(x) = V''(\phi_S(x)) = 1 - \frac{3}{\cosh^2 \frac{1}{2}x}. \quad (25)$$

$U$  is a Pöschl–Teller potential, so the solutions of eq.(24) are well known. There are three (normalised) discrete modes,

$$\eta_{-1}(x) = \sqrt{\frac{15}{32}} \frac{1}{\cosh^3 \frac{1}{2}x}, \quad \omega_{-1}^2 = -\frac{5}{4}, \quad (26)$$

$$\eta_0(x) = \sqrt{\frac{15}{8}} \frac{\sinh \frac{1}{2}x}{\cosh^3 \frac{1}{2}x}, \quad \omega_0^2 = 0, \quad (27)$$

$$\eta_1(x) = \sqrt{\frac{3}{32}} \frac{4 \cosh^2 \frac{1}{2}x - 5}{\cosh^3 \frac{1}{2}x}, \quad \omega_1^2 = \frac{3}{4}. \quad (28)$$

The presence of a unique unstable mode  $\eta_{-1}$  with negative squared frequency means that the lump is a sphaleron. It is the saddle point in field configuration space between the false vacuum  $\phi \equiv 0$  (with zero energy) and configurations with negative energy, whose field  $\phi$  is large and positive in some region of physical space. After being perturbed in the unstable direction towards the false vacuum, the sphaleron's evolution connects it with the oscillon. The sphaleron's discrete shape mode  $\eta_1$ , whose positive frequency  $\omega_1$  is below the continuum threshold at  $\omega = 1$ , is also important. It is the source of a second degree of freedom for the oscillon.  $\eta_0$  is the translation zero mode, and can be ignored here, because it has the opposite

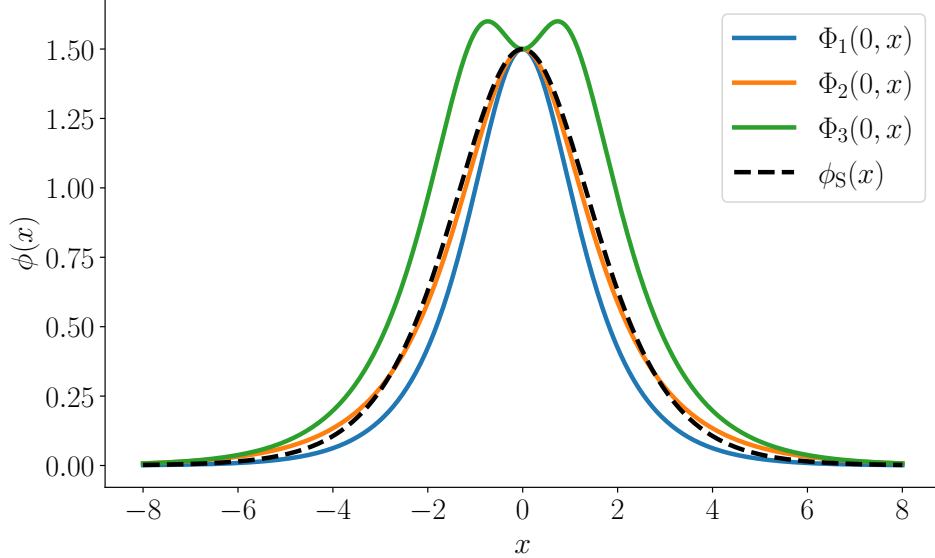


FIG. 5: Match between the sphaleron  $\phi_S(x)$  and the profiles  $\Phi_N(0, x)$  for optimal  $\epsilon$ .

reflection symmetry to the other modes, and doesn't contribute to an oscillon whose centre of mass is at rest.

It is instructive to compare the truncated oscillon profiles  $\Phi_N(0, x)$  for varying  $\epsilon$  with the sphaleron profile (FIG. 5).  $\Phi_1(0, 0)$  matches the sphaleron central amplitude  $\phi_S(0) = \frac{3}{2}$  for  $\epsilon = \frac{3}{2}\sqrt{\frac{5}{12}} \approx 0.9682$ . This corresponds to an oscillon frequency  $\omega = \frac{1}{4}$ . However, the  $L^2$  norm  $\|\phi_S(x) - \Phi_1(0, x)\|^2 \approx 0.1776$  shows that the match of profiles is not good. The second truncation matches much better. The condition  $\Phi_2(0, 0) = \frac{3}{2}$  is a quadratic equation with solutions

$$\epsilon_1 = \frac{15 - 5\sqrt{3}}{4\sqrt{5}} \approx 0.7088, \quad \epsilon_2 = \frac{-15 - 5\sqrt{3}}{4\sqrt{5}} \approx -2.6453. \quad (29)$$

The second solution is outside the acceptable range,  $-1 < \epsilon < 1$ , but the first gives a profile very close to the sphaleron with  $\|\phi_S(x) - \Phi_2(0, x)\|^2 \approx 0.0138$ . The corresponding oscillon frequency is  $\omega \approx 0.7054$ .  $\Phi_3$  has a profile with a dip for large  $\epsilon$  and matches much worse, as does  $\Phi_4$ .

## V. COLLECTIVE COORDINATE MODEL BASED ON THE SPHALERON

Reflection-symmetric field evolution around the sphaleron, including the (normalised) unstable and shape modes  $\eta_{-1}$  and  $\eta_1$ , can be modelled by the ansatz

$$\phi(t, x) = \phi_S(x) + A(t)\eta_{-1}(x) + B(t)\eta_1(x). \quad (30)$$

At the linearised level,  $B$  oscillates and  $A$  tends to grow exponentially, suggesting that the ansatz will be valid for limited time. Rather surprisingly, this ansatz has an extended approximate validity.  $A$  and  $B$  can be assumed to have unconstrained magnitudes, and can be treated as collective coordinates of the field  $\phi$ . Their nonlinear time-evolution gives an approximate model for the oscillon. To find the model equations, we substitute the ansatz (30) into the field Lagrangian (1). After evaluating the derivatives and integrating over space (and discarding boundary terms), we obtain a reduced, effective Lagrangian whose nonlinear equations of motion define the collective coordinate dynamics.

Because the discrete modes are localised, they provide a useful approximation to the oscillon. This is especially true for oscillons whose amplitude is not too small. Recall that an oscillon of small amplitude has a large spatial extent (since in the Fodor et al. analysis it is a function of the scaled spatial variable  $\zeta = \epsilon x$ ). Oscillons of larger amplitude have a shape closer to that obtained by deforming the sphaleron by its discrete modes.

The reduced Lagrangian is of the form

$$L_{\text{eff}}[A, B] = \frac{1}{2}\dot{A}^2 + \frac{1}{2}\dot{B}^2 - V_{\text{eff}}(A, B), \quad (31)$$

where overdots are now unscaled time-derivatives and

$$V_{\text{eff}}(A, B) = \frac{6}{5} - \frac{5}{8}A^2 + \frac{3}{8}B^2 - C_1A^3 - C_2A^2B - C_3AB^2 - C_4B^3, \quad (32)$$

with the constants  $C_1, \dots, C_4$  given below. To establish this, some integration by parts is needed, together with use of the nonlinear equation satisfied by  $\phi_S$  and the linearised equations for the retained modes. The kinetic terms have a simple Euclidean form because the modes are orthonormal. The first three coefficients in the potential  $V_{\text{eff}}$  are the energy of the sphaleron and half the (negative and positive) squared frequencies of the retained modes. The coefficients of the cubic terms are the integrals

$$\begin{aligned} C_1 &= \frac{1}{3} \int_{-\infty}^{\infty} \eta_{-1}^3(x) dx = \sqrt{\frac{15}{2}} \frac{175\pi}{8192}, & C_2 &= \int_{-\infty}^{\infty} \eta_{-1}^2(x)\eta_1(x) dx = -\sqrt{\frac{3}{2}} \frac{225\pi}{8192}, \\ C_3 &= \int_{-\infty}^{\infty} \eta_{-1}(x)\eta_1^2(x) dx = \sqrt{\frac{15}{2}} \frac{129\pi}{8192}, & C_4 &= \frac{1}{3} \int_{-\infty}^{\infty} \eta_1^3(x) dx = \sqrt{\frac{3}{2}} \frac{201\pi}{8192}. \end{aligned} \quad (33)$$

From the reduced Lagrangian (31) we obtain the equations of motion

$$\frac{d^2 A}{dt^2} = \frac{5}{4}A + 3C_1A^2 + 2C_2AB + C_3B^2, \quad (34a)$$

$$\frac{d^2 B}{dt^2} = -\frac{3}{4}B + C_2A^2 + 2C_3AB + 3C_4B^2. \quad (34b)$$

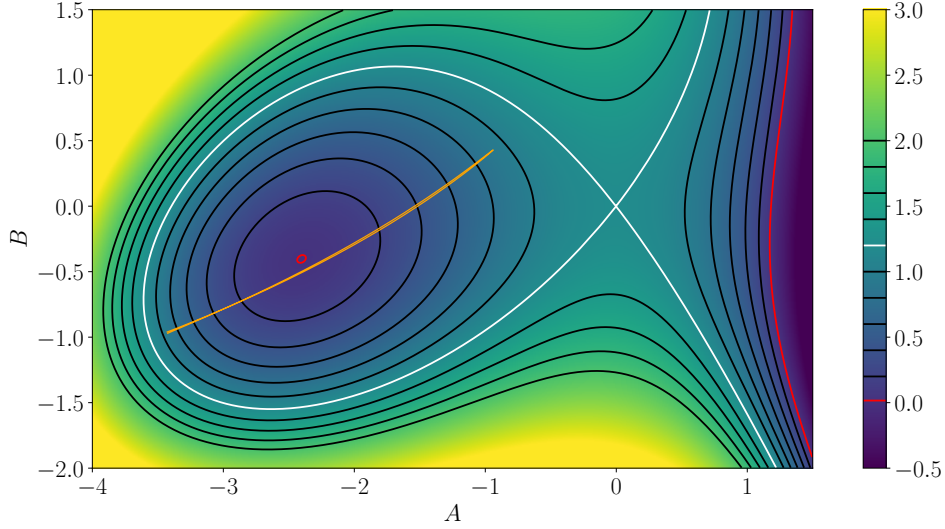


FIG. 6: Effective potential  $V_{\text{eff}}(A, B)$ . The white contour corresponds to the energy 1.2 of the sphaleron and the pair of red contours to energy 0.016, slightly above that of the approximate (false) vacuum. The orange line is a trajectory of a solution discussed in section VI and FIG. 13.

and the conserved energy

$$E_{\text{eff}}[A, B] = \frac{1}{2}\dot{A}^2 + \frac{1}{2}\dot{B}^2 + V_{\text{eff}}(A, B), \quad (35)$$

FIG. 6 shows a contour plot of  $V_{\text{eff}}$ . There is a saddle point at  $A = B = 0$  corresponding to the sphaleron, and a local minimum at  $A = -2.40501, B = -0.40325$  corresponding to an approximation to the (false) vacuum  $\phi \equiv 0$ , whose energy is 0.01532 and whose field configuration (30) is shown in FIG. 7. In the reduced dynamics, diagonalised small perturbations around the approximate vacuum have frequencies  $\tilde{\omega}_1 = 1.02216$  and  $\tilde{\omega}_2 = 1.37920$ , which are above the continuum threshold frequency  $\omega = 1$ . This is partly because the minimum is not the exact vacuum, but mainly because the perturbations are linear combinations of the localised modes  $\eta_{-1}$  and  $\eta_1$ , which do not have the large wavelengths of radiation modes close to the threshold.

We have explored the extent to which important features of a solution  $\phi(t, x)$  of the field equation (2) are captured by this reduced model. To do this it is useful to follow the amplitudes of the projection of  $\phi$  onto the modes  $\eta_{-1}$  and  $\eta_1$ ,

$$A_p(t) = \int_{-\infty}^{\infty} (\phi(t, x) - \phi_S(x)) \eta_{-1}(x) dx, \quad B_p(t) = \int_{-\infty}^{\infty} (\phi(t, x) - \phi_S(x)) \eta_1(x) dx. \quad (36)$$

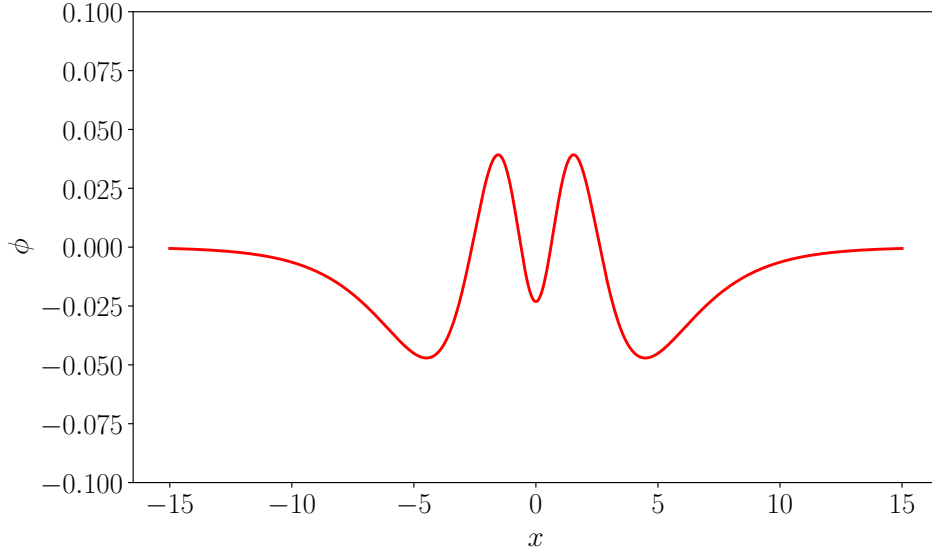


FIG. 7: Optimal approximation to the (false) vacuum configuration using the sphaleron plus modes expansion (30).

Because the modes are orthogonal to each other and to the radiation, this method is equivalent to the usual least squares fit of  $\phi$  to the function (30), but it is numerically faster and more stable. FIG. 8 illustrates this approach for the numerical field evolution of a perturbed sphaleron, with initial condition  $\phi(0, x) = \phi_S(x) - 0.001\eta_{-1}(x)$ , decaying to an oscillon, and FIG. 9 is for the evolution from the truncated Fodor et al. series  $\phi(0, x) = \Phi_4(0, x)$  with  $\epsilon = 0.5$  as initial condition. The upper-left plots a) show the values of the projected mode amplitudes  $A_p, B_p$  and the  $L^2$  norm of the remainder  $\|\delta\phi\|^2$ . The upper-right plots b) show the comparison between the field value  $\phi(t, 0)$  at the centre (orange line) and its approximation  $\Phi_4(t, 0)$  (blue line). The lower-left plots c) show the energy  $\mathcal{E}(|x| < 8)$  within the interval  $-8 < x < 8$  of the solution  $\phi(t, x)$  and the energy of the reduced model  $E(A_p, B_p)$  for the fitted  $A_p(t), B_p(t)$  values. The lower-right plots d) compare the field profiles  $\phi(t, x)$  at the time  $t = T_{\max}$  of the last maximum of  $\phi(t, 0)$  before  $t = 50$  (green) and its projection (red).

In the case of sphaleron decay (FIG. 8), the oscillon is initially generated with a large amplitude, but this soon reduces. The field is accurately approximated only until  $\phi(t, 0)$  crosses zero for the first time. Then the remainder grows and the energy in the projected modes starts to decrease (unlike in the reduced model itself). Energy starts to escape from the interval  $-8 < x < 8$  in less than 20 time-units, and converts to radiation. This is

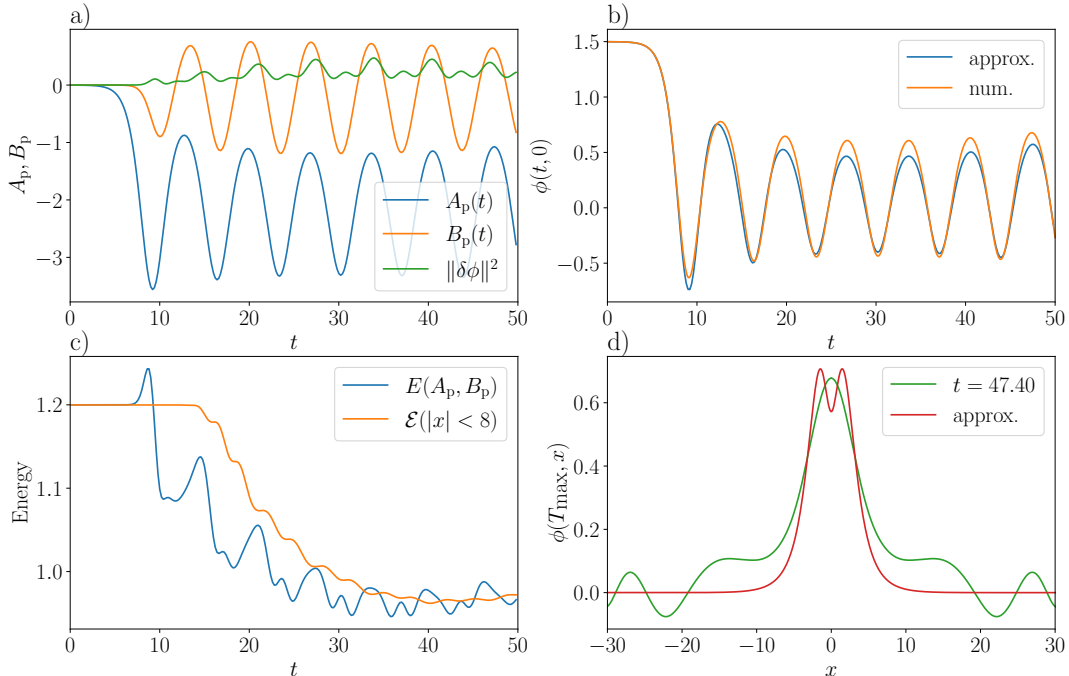


FIG. 8: Evolution from initial condition  $\phi(0, x) = \phi_S(x) - 0.001\eta_{-1}(x)$  compared with the projected mode parameters of the effective model.

confirmed by the field profile at the latest maximum where radiation with an amplitude approximately 0.1 is clearly visible.

Starting from the Fodor et al. configuration  $\Phi_4$  with smaller initial amplitude (FIG. 9), substantially less energy is lost and all the parameters are much better approximated. The energy decreases by about 5% within the simulation time, compared to over 20% during sphaleron decay. We expect that at a later stage of oscillon evolution, or from more carefully prepared initial conditions, radiation would be even less. This is confirmed below.

## VI. COMPARISON OF OSCILLON MODELS

It is particularly interesting to look at the trajectory of the reduced dynamics that starts just slightly perturbed from the sphaleron saddle point in either direction of the unstable mode. This is shown in FIG. 10. A positive perturbation leads to field blow-up, and a negative perturbation leads to oscillon formation. In both cases, starting from the same initial conditions, the full field dynamics (solid lines) is captured well by the reduced model (dashed lines) in its initial stages. In the case of oscillon formation, however, radiation



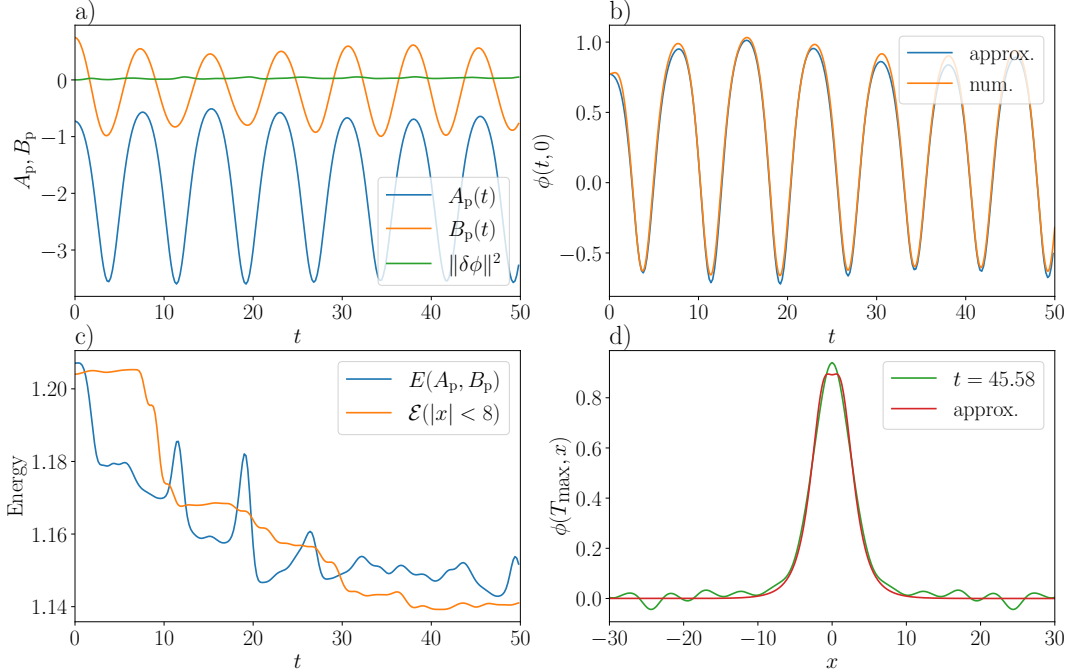


FIG. 9: Evolution from initial condition  $\phi(0, x) = \Phi_4(0, x)$  for  $\epsilon = 0.5$  compared with the projected mode parameters of the effective model.

production results in a separation of trajectories. The reduced dynamics is quasiperiodic and almost returns to the initial amplitude  $\phi(0, 0) = 1.499$  at  $t \approx 60$ . The full field dynamics near  $x = 0$  becomes almost quasiperiodic from  $t \approx 15$  onwards, but it has a smaller amplitude oscillating between 0.55 and 0.7, and a higher basic frequency  $\omega = 0.9024$ . Both solutions for longer times are shown in FIG. 11. The difference is particularly visible for initial data for which an oscillon does not form. An example of such evolution is shown in FIG. 12. Again, at the initial stage, during the first oscillation, the field and reduced dynamics are very similar. But later the field dynamics is dominated by radiation.

The best match between the field dynamics and the dynamics of the reduced model occurs for initial data where a true oscillon is produced with minimal transient radiation. We have found such an oscillon for  $A(0) = -3.4247$ ,  $B(0) = -1.0218$ . The evolution is shown in FIG. 13. The field and reduced dynamics are very close, except for a small difference in frequencies. However, at later times it is clear that the field and reduced dynamics do differ. The field dynamics is almost periodic with  $\omega = 0.9024$  and minimum field value  $\phi_{\min} = -0.5211$ , whereas the reduced dynamics is visibly quasiperiodic (bottom panel centre) with the field minimum oscillating between  $-0.59$  and  $-0.53$ . This is because the field dynamics always

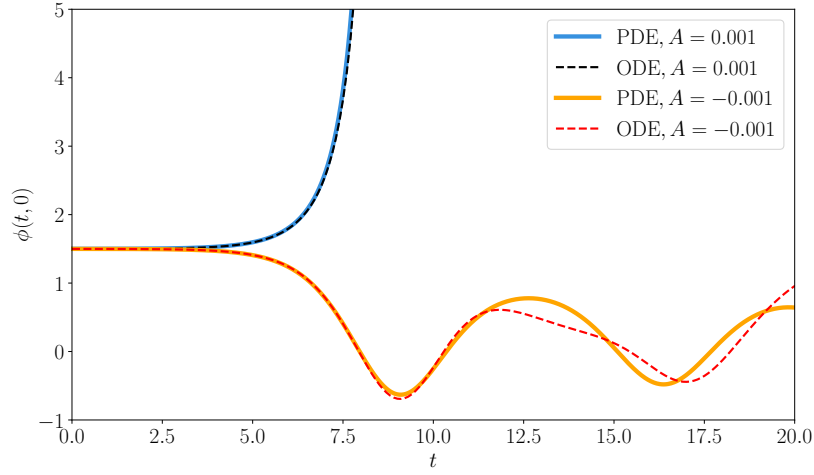


FIG. 10: Solutions of the field equation (PDE) and reduced equations (ODEs) for initial conditions  $\phi(0, x) = \phi_S(x) + A\eta_{-1}(x)$ .

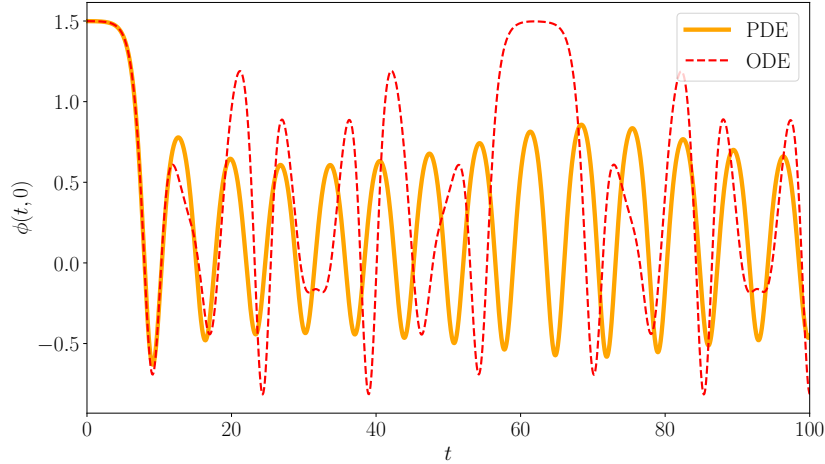


FIG. 11: Longer-time solutions of the field equation (PDE) and reduced equations (ODEs) for initial conditions  $\phi(0, x) = \phi_S(x) - 0.001\eta_{-1}(x)$ .

produces some radiation, especially early on, so the oscillon settles into a slightly different state. But by analysing solutions of the reduced model we have found initial conditions where the solution  $\phi$  is periodic with amplitude  $\phi_{\min} = -0.5485$  and frequency  $\omega^* = 0.8967$ , very similar to the oscillon in the field theory. This periodic solution is also shown in FIG. 13, and shown in the  $(A, B)$  plane in FIG. 6 (orange line).

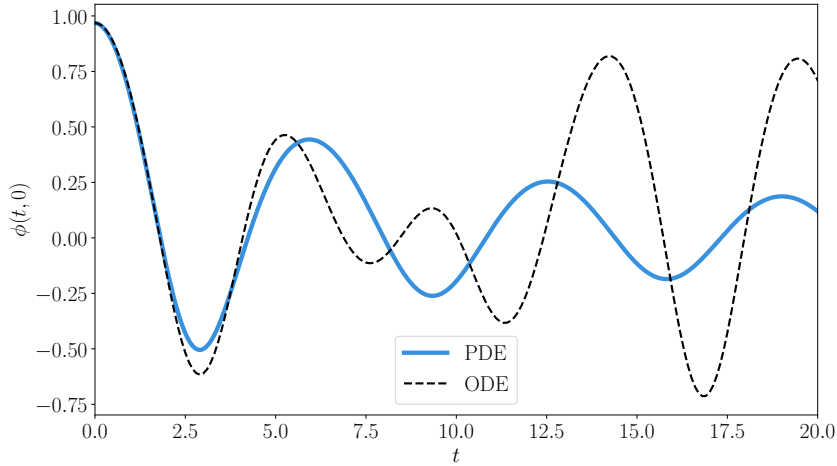


FIG. 12: Solutions of the field equations (PDE) and reduced equations (ODEs) for initial conditions corresponding to a substantially deformed sphaleron with

$$A(0) = -1, B(0) = -0.5.$$

By following sphaleron decay in the field theory for an even longer time, we see that the beats persist with slightly smaller amplitude (FIG. 14). The main frequency increases to  $\omega \approx 0.913$  at  $t \approx 2000$ . The field shape remains lump-like but grows slightly wider (FIG. 15). FIG. 16 shows the power spectrum of the field  $\phi(t, x)$ . It reveals the main frequency at  $\omega = 0.9075$  and its harmonics. The higher harmonics are widened due to the frequency drift with time. Around each main peak there is a family of equidistant smaller peaks. Their positions correspond very well with  $|n_1\omega + n_2|$ , which shows that there is another basic frequency near the threshold  $m = 1$ . These peaks are generated by resonances due to the nonlinearity of the field equation. Recall that the reduced model has quasi-periodic solutions but neither of the frequencies is very close to 1.

Not all initial conditions of the sphaleron modes ansatz (30) give oscillons immediately, as we have seen; one needs to minimise the energy loss to radiation, (22). We have found the values of  $A$  and  $B$  achieving this for a range of initial central amplitudes  $\phi_0 = \phi(0, 0)$ . We have also investigated the subsequent energy loss as a function of  $\phi_0$ . For  $\phi_0 > 0.8$  the ansatz (30) gives as good an initial condition as the best initial condition  $\Phi_2$  from the Fodor et al. expansion. Moreover, the reduced model reproduces the amplitude decay very well, at least up to the first minimum of the field profile, whereas  $\Phi_2$  evolves strictly periodically. The

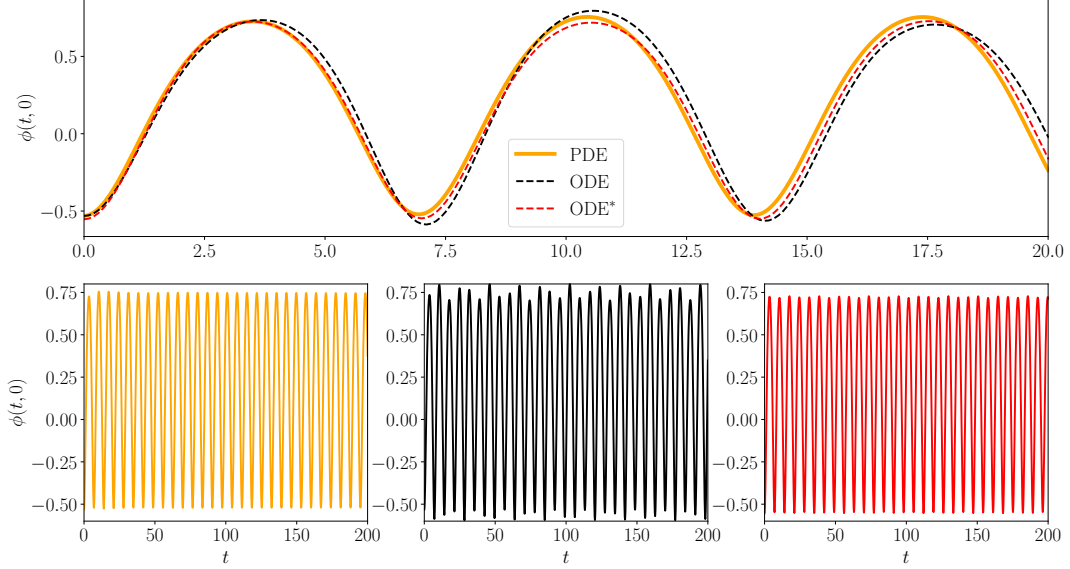


FIG. 13: Solutions of the field equation (PDE) and reduced equations (ODEs) for initial conditions corresponding to the sphaleron modes ansatz with  $A(0) = -3.4247$ ,  $B(0) = -1.0218$ . The red line (ODEs\*) is the periodic solution of the reduced equations with  $A^*(0) = -3.4287$ ,  $B^*(0) = -0.9605$ .

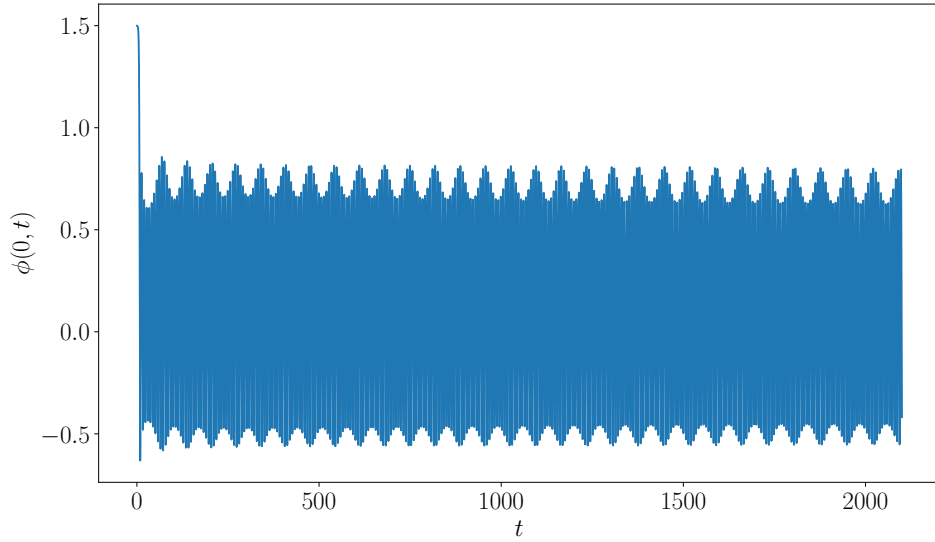


FIG. 14: Approximately quasi-periodic oscillation arising from sphaleron decay with initial condition  $\phi(0, x) = \phi_S(x) - 0.001\eta_{-1}(x)$ .

reduced model has more degrees of freedom and has other types of solution, one example of which will be presented in the following section.

Further evidence that there is an overlap between these two approximations is shown in

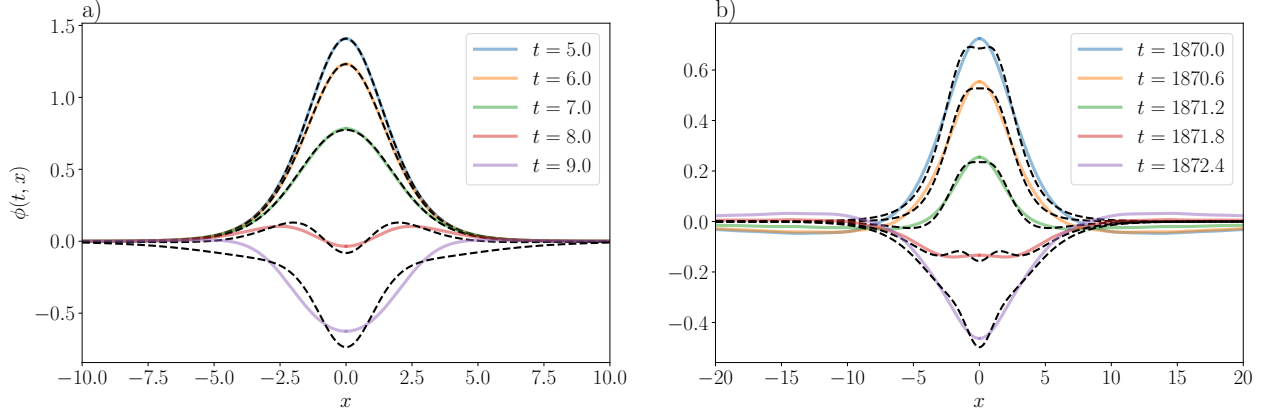


FIG. 15: Decomposition of a field profile (colour lines) into sphaleron and its modes (dashed lines) a) at the initial stage of evolution and b) at a much later time.

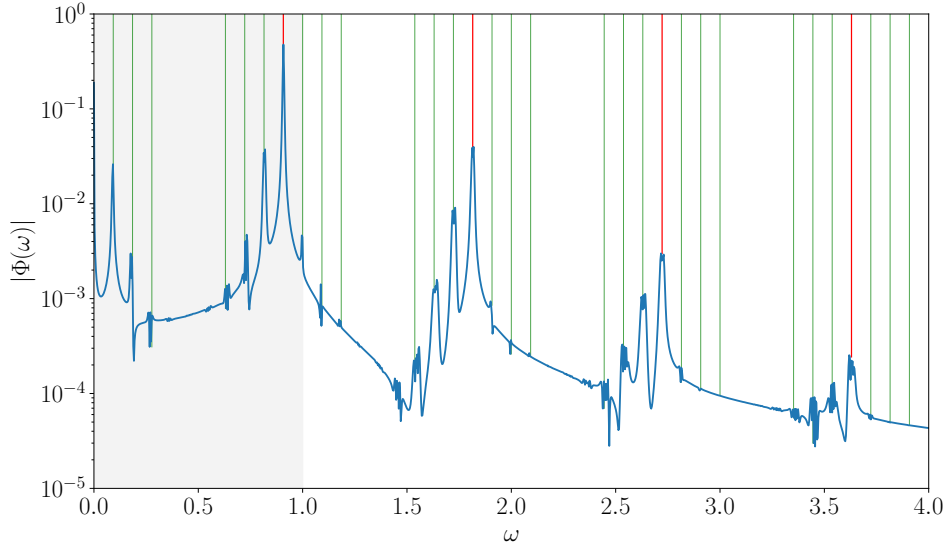


FIG. 16: Power spectrum of field at center for  $100 < t < 2000$ . Red lines indicate harmonics of the primary frequency  $\omega = 0.9075$ , the thin green lines indicate some of the combinations  $|n_1\omega + n_2|$  for  $-3 \leq n_2 \leq 3$ . The widening of the peaks is due to a slow frequency drift.

FIG. 17, where on the  $(A, B)$  plane we have plotted the points corresponding to the minimal energy loss  $\Delta E$  and the projection coefficients of  $\Phi_2$  on to the modes  $\eta_{-1}$  and  $\eta_1$ . Note that these projections do not make much sense for small values of  $\epsilon$  because the oscillon is much wider than the sphaleron and its discrete modes. An interesting observation can be made regarding  $\Phi_2$  which lies very close to the points of minimal energy loss. Its evolution for  $\epsilon = 0.728$  passes close ( $A = -0.016, B = -0.027$ ) to the sphaleron with  $A = B = 0$ . Some

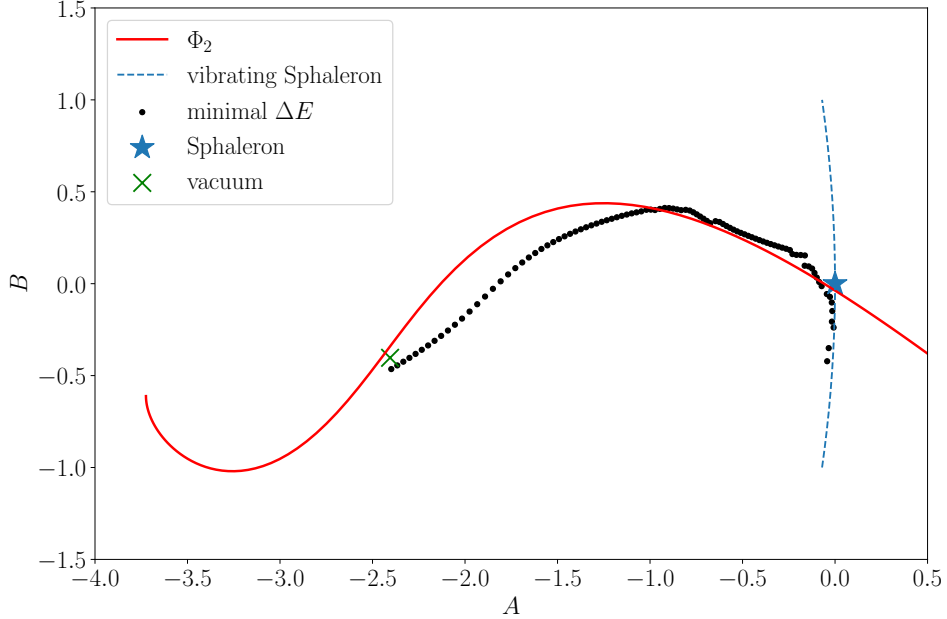


FIG. 17: Comparison of the initial conditions leading to the lowest energy loss for given  $\phi_0$  (black dots) and the  $\Phi_2$  approximation for  $\epsilon \in [-0.95, 0.95]$  (red line), projected on to the sphaleron modes. Static solutions for the sphaleron and approximate vacuum are also marked along with the solution corresponding to the vibrating sphaleron.

points obtained by minimising the energy loss also lie very close to the line corresponding to the vibrating sphaleron, which we discuss next.

## VII. VIBRATING SPHALERON

At the linearised level of the reduced model, with Lagrangian (31), the shape mode  $\eta_1$  of the sphaleron oscillates indefinitely with constant amplitude  $\mathcal{B}$  and frequency  $\omega_1 = \sqrt{3/4}$ . However, the nonlinear coupling of  $B$  to  $A$  leads to an excitation of the unstable mode  $\eta_{-1}$  as well. In eq.(34a), the term  $C_3 B^2$  can cause exponential growth of  $A$ . We see this in more detail by solving eqs.(34a, 34b) to low order in  $\mathcal{B}$ . Assume that at linear order only the shape mode is excited, so

$$A(t) = 0, \quad B(t) = \mathcal{B} \cos(\omega_1 t). \quad (37)$$

At quadratic order,

$$\frac{d^2 A}{dt^2} = \frac{5}{4}A + C_3 B^2 = \frac{5}{4}A + \frac{1}{2}C_3 \mathcal{B}^2 + \frac{1}{2}C_3 \mathcal{B}^2 \cos(2\omega_1 t), \quad (38)$$

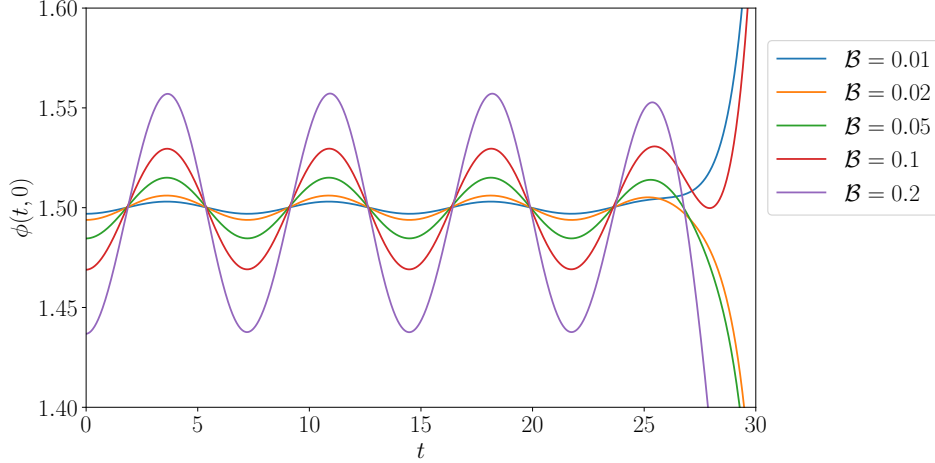


FIG. 18: Nearly periodic evolution of the vibrating sphaleron with fine-tuned initial data.

whose general solution is

$$A(t) = F_1 e^{|\omega_{-1}|t} + F_2 e^{-|\omega_{-1}|t} - C_3 \mathcal{B}^2 \left( \frac{2}{5} + \frac{2}{5 + 16\omega_1^2} \cos(2\omega_1 t) \right), \quad (39)$$

where  $|\omega_{-1}| = \sqrt{5/4}$ .

Generally,  $F_1$  is non-zero and the solution grows exponentially. However, for the initial conditions

$$\frac{dA}{dt}(0) = 0, \quad A(0) = -C_3 \mathcal{B}^2 \left( \frac{2}{5} + \frac{2}{5 + 16\omega_1^2} \right) = -\frac{44}{85} C_3 \mathcal{B}^2 \quad (40)$$

there are no exponential terms in the solution, and only constant and oscillatory terms remain. Motivated by this, we have fine-tuned the initial conditions in the field theory and obtained an almost periodic, vibrating sphaleron with a varying amplitude of oscillation, as shown in FIG. 18. For initial conditions we took

$$\phi_t(0, x) = 0, \quad \phi(0, x) = \phi_S(x) - \alpha \frac{44}{85} C_3 \mathcal{B}^2 \eta_{-1}(x) + \mathcal{B} \eta_1(x), \quad (41)$$

where  $\alpha$  was chosen to suppress exponential growth for as long as possible.  $\alpha = 1.024$  for  $\mathcal{B} = 0.2$  and  $\alpha$  decreases to 1 as  $\mathcal{B}$  approaches 0. Similar vibrating sphaleron solutions were considered earlier at linear order in [10].

## VIII. CONCLUSIONS

We have considered a simple 1-dimensional scalar field theory with a cubic potential, having a long-lived oscillon solution as well as a static, unstable sphaleron solution. We

have explicitly constructed the Fodor et al. expansion for the oscillon up to fourth order in the oscillon's amplitude parameter. As this parameter increases, the oscillon frequency decreases. The expansion is asymptotic rather than convergent, so the fourth-order truncation  $\Phi_4(t, x)$  is only valid for small amplitudes. A larger-amplitude oscillon is better approximated by the second-order truncation  $\Phi_2(t, x)$ .

When the oscillon is instantaneously at rest, its shape is similar to that of the sphaleron, but the sphaleron has larger amplitude and more energy. The sphaleron, slightly perturbed, decays into the oscillon. During its first couple of oscillations it radiates a significant fraction of its energy, but then settles into an oscillon of relatively large amplitude.

The Fodor et al. oscillon is periodic, with a single fundamental frequency. However, the decaying sphaleron approaches an oscillon whose amplitude is itself slightly oscillating. This suggests that oscillon solutions are best modelled by a truncation of the field theory having two degrees of freedom. The sphaleron naturally provides these – it has a single unstable mode and a further discrete mode of oscillation whose frequency is below the threshold frequency for the continuum of radiation modes.

We have considered the field ansatz obtained by linearly deforming the sphaleron by these two modes, with amplitudes  $A$  and  $B$ . Substituting this ansatz into the full field-theory Lagrangian, we obtain a reduced, nonlinear dynamical Lagrangian for  $A$  and  $B$ , whose nonlinearity arises from the cubic potential term. This dynamics is decoupled from the field radiation modes. Because the ansatz gets quite close to the vacuum configuration for particular values of  $A$  and  $B$ , it provides a useful interpolation between the sphaleron and the vacuum. The dynamical equations for  $A$  and  $B$  have solutions describing sphaleron decay as well as oscillons of relatively large amplitude. However, oscillons of small amplitude, which have a larger spatial extent than the sphaleron and its discrete modes, are not well-described by the ansatz.

By carefully adjusting the initial conditions of  $A$  and  $B$ , we can find oscillatory solutions of the reduced dynamics that are almost exactly periodic. We can also use these initial conditions as initial conditions for the field theory itself, to generate oscillons with minimal radiation. We then find close similarities between the field theory dynamics and the reduced dynamics of  $A$  and  $B$ . The comparison is effected by projecting the field dynamics on to the two discrete modes.

In summary, we have found similar oscillon solutions from several points of view –



through the Fodor et al. small-amplitude expansion, through the decay of the sphaleron and oscillating versions of the sphaleron, and from our truncation of the field theory to a dynamical system with two degrees of freedom. This dynamical system appears to be a useful extension of the truncation to one degree of freedom implied by the Fodor et al. analysis. However, all these approaches are only approximate. The Fodor et al. expansion is asymptotic and needs to be truncated; the decaying sphaleron emits considerable radiation in its initial few oscillations; finally, our linearised field ansatz exploiting the sphaleron's discrete modes misses the vacuum and small-amplitude oscillons.

Numerically, there is overwhelming evidence for the existence of long-lived, topologically-trivial, localised oscillatory solutions of the field theory – oscillons – but the precise mathematical status of oscillons remains elusive.

### ACKNOWLEDGEMENTS

The research of TR was supported by the Polish National Science Centre, grant number NCN 2019/35/B/ST2/00059.

- 
- [1] M. Gleiser and D. Sicilia, *Phys. Rev. D* **80**, 125037 (2009), [arXiv:0910.5922 \[hep-th\]](#).
  - [2] F. R. Klinkhamer and N. S. Manton, *Phys. Rev. D* **30**, 2212 (1984).
  - [3] P. Dorey, T. Romańczukiewicz, and Y. Shnir, *Phys. Lett. B* **806**, 135497 (2020), [arXiv:1910.04128 \[hep-th\]](#).
  - [4] G. Fodor, P. Forgács, Z. Horváth, and A. Lukács, *Phys. Rev. D* **78**, 025003 (2008), [arXiv:0802.3525 \[hep-th\]](#).
  - [5] J. K. Perring and T. H. R. Skyrme, *Nucl. Phys.* **31**, 550 (1962).
  - [6] P. Dorey, A. Gorina, I. Perapechka, T. Romańczukiewicz, and Y. Shnir, *JHEP* **09**, 145 (2021), [arXiv:2106.09560 \[hep-th\]](#).
  - [7] C. G. Callan, Jr. and S. Coleman, *Phys. Rev. D* **16**, 1762 (1977).
  - [8] A. T. Avelar, D. Bazeia, L. Losano, and R. Menezes, *Eur. Phys. J. C* **55**, 133 (2008), [arXiv:0711.4721 \[hep-th\]](#).
  - [9] F. Blaschke and O. N. Karpíšek, *PTEP* **2022**, 103A01 (2022), [arXiv:2202.05675 \[hep-th\]](#).

- [10] P. Bizoń, T. Chmaj, and N. Szpak, *J. Math. Phys.* **52**, 103703 (2011), [arXiv:1012.1033 \[math-ph\]](#).